OPEN

Dihydroartemisinin Attenuates Hypoxia-Induced Pulmonary Hypertension Through the ELAVL2/miR-503/PI3K/AKT Axis

Haijian Cai, MD, Shiqian Fan, MD,*† Luqiong Cai, MBBS,* Lin Zhu, MBBS,* Zhucheng Zhao, MBBS,* Yaozhe Li, MD,* Yizhu Yao, MBBS,* Xiaoying Huang, PhD,* and Liangxing Wang, PhD**

Abstract: Dihydroartemisinin (DHA) is an active form of artemisinin extracted from the traditional Chinese medicine *Artemisia annua*, which is used to treat malaria. Previous studies have shown that DHA has a therapeutic effect on pulmonary hypertension (PH), but its specific mechanism has not been fully elucidated. In this study, a hypoxia-induced PH mouse model was established and DHA was administered as a therapeutic intervention. We measured hemodynamics and right ventricular hypertrophy and observed hematoxylin and eosin staining of lung tissue sections, proving the therapeutic effect of DHA on PH. Furthermore, cell counting kit-8 and 5-ethynyl-2′-deoxyuridine (EdU) cell proliferation assay kit were performed to examine cell proliferation of pulmonary artery smooth muscle cells cultured in hypoxia or in normoxia. Transwell migration chamber assay was performed to examine cell migration of the same cell model. Consistent with the therapeutic effect in vivo, DHA inhibited hypoxia-induced cell proliferation and migration. Through high-throughput sequencing of mouse lung tissue, we screened embryonic lethal abnormal vision-like 2 (ELAVL2) as a key RNA binding protein in PH. Mechanistically, DHA inhibited the proliferation and migration of pulmonary artery smooth muscle cells by promoting the expression of ELAVL2 and regulating the miR-503/PI3K/AKT pathway. The binding relationship between ELAVL2 and pre-miR-503 was verified by RNA binding protein immunoprecipitation assay. In conclusion, we first propose that DHA alleviates PH through the ELAVL2/miR-503/PI3K/AKT pathway, which may provide a basis for new therapeutic strategies of PH.

Received for publication January 18, 2022; accepted March 18, 2022.

From the *Division of Pulmonary Medicine, The First Affiliated Hospital of Wenzhou Medical University, Key Laboratory of Heart and Lung, Wenzhou, Zhejiang, China; and †Yiwu Hospital Affiliated to Wenzhou Medical University (Yiwu Municipal Central Hospital), Yiwu, Zhejiang, China.

The authors report no conflicts of interest.

H. Cai, S. Fan, and L. Cai have contributed equally to this work.

H. Cai, S. Fan, X. Huang, and L. Wang designed experiments and wrote the manuscript. H. Cai, S. Fan, L. Cai, and L. Zhu conducted experiments. H. Cai, S. Fan, L. Cai, Z. Zhao, and Y. Li collected the data and participated in statistical analyses. All authors have read and approved the final manuscript.

Correspondence: Xiaoying Huang, PhD or Liangxing Wang, PhD (e-mail: huangxiaoying@wzhospital.cn or wangliangxing@wzhospital.cn).

Key Words: dihydroartemisinin, pulmonary hypertension, hypoxia, MiR-503, ELAVL2

(*J Cardiovasc Pharmacol*™ 2022;80:95–109)

INTRODUCTION

Pulmonary hypertension (PH) is a chronic disease characterized by dysfunction of pulmonary artery endothelial cells (PAECs), abnormal proliferation of pulmonary artery smooth muscle cells (PASMCs), and remodeling of the vascular structure, ultimately leading to heart failure and death.[1,2] Vascular remodeling is a particularly important and prevalent step in the progression of PH, which ultimately leads to severe adverse outcomes.[3]

PH pathogenesis involves multiple interrelated factors. Imbalances in transcription,[4] post-transcriptional modification,[5] translation,[6] and post-translational modification[7] have all been found to be involved in the development of PH. These steps are key to the abnormal proliferation of PASMCs. Further exploration of the regulatory mechanisms that affect the proliferation and migration of PASMCs is expected to provide new therapeutic targets for treatment.

One promising molecule that may be applicable to PH is dihydroartemisinin (DHA), the main active form of artemisinin, an extract of the herb *Artemisia annua*.[8] DHA has been shown to have beneficial effects on cell proliferation,[9] ferroptosis,[10] autophagy,[11] apoptosis,[12] and other disease-associated processes. Specifically, DHA has been reported to reduce mean pulmonary arterial pressure in rats with monocrotaline (MCT)-induced PH and inhibit the proliferation of PASMCs and PAECs.[13,14] However, the mechanisms by which DHA exerts its anti-vascular remodeling effect in PH, especially in PASMCs, have not been fully elucidated.

A potential target of DHA in this regard is embryonic lethal abnormal vision-like 2 (ELAVL2), which is a member of the ubiquitous ELAVL protein family of RNA binding proteins (RBPs).[15] ELAVL2 is composed of 3 conserved RNA recognition motifs (RRMs), the first 2 of which (RRM1 and RRM2) have been shown to bind directly to transcripts containing AU-rich elements.[16] Notably, ELAVL2 overexpression inhibits the proliferation of neuronal stem cells.[17] This suggests that this protein may also be involved in the mechanisms underlying PASMC proliferation. Increasing studies have shown that the interaction and cooperation between RBPs and microRNAs

(miRNAs) is one of the keys in post-transcriptional regulation. Interestingly, ELAVL2 was found to interact with more than 50 miRNA precursors in a 2017 study, which means ELAVL2 has great potential in regulating miRNAs.[18]

miRNAs are a class of noncoding nucleotide sequences with a length of approximately 22 nucleotides that can negatively regulate the stability of mRNA at the post-transcriptional level.[19] Studies have shown that the overexpression of miR-503 can inhibit MCT-induced PH in rats.[20] In mouse pulmonary fibrosis models, miR-503 can reduce silica-induced pulmonary fibrosis by down-regulating the expression of PI3K.[21] Under hypoxic conditions, the PI3K-AKT signaling pathway is activated, which contributes to the proliferation of PASMCs.[22] Therefore, we hypothesized that the activation of ELAVL2/miR-503 could inhibit the PI3K-AKT axis under hypoxia.

In this study, we demonstrated that DHA inhibited the proliferation of PASMCs by promoting the expression of ELAVL2. The inhibition of proliferation and migration was shown to depend on the regulation of the miR-503/PI3K/AKT axis by ELAVL2. These findings provide a theoretical basis for identifying new targets for the treatment of PH.

MATERIALS AND METHODS

Reagents

DHA was purchased from TCI (Tokyo, Japan). The rabbit anti-ELAVL2 antibody (1:1000, #DF3251) used for western blotting was purchased from Affinity (USA) and the rabbit anti-ELAVL2 antibody (3.5 μg, #14008-1-AP) used for the RNA-binding protein immunoprecipitation assay was purchased from Proteintech (Chicago, IL). Rabbit antibodies recognizing β-actin (1:1000, #4970), PCNA (1:1000, #13110), PI3K (1:1000, #4292), AKT (1:1000, #4691), and phosphorylated AKT (p-AKT) (1:1000, #4060S) were obtained from Cell Signaling Technology (Beverly, MA). Horseradish peroxidase -conjugated goat antirabbit IgG (1:10,000, #BL003A) were obtained from Biosharp (Hefei, China). The PI3K agonist 740Y-P (S7865) and PI3K inhibitor LY294002 (S1105) were purchased from Selleck (Shanghai, China).

Animal Models

Male C57BL/6 mice (approximately 10 weeks old, 20–25 g) were purchased from the Vital River Laboratory Animal Technology (Beijing, China). The experimental scheme and animal housing procedures were approved by the Animal Ethics Committee of the Wenzhou Medical University. The mice were randomly divided into 4 groups: a normoxic group (nor; treated with saline), a hypoxic group (hyp; treated with saline), a hypoxic group treated with a low dose of DHA (hyp/DHA; 45 mg/kg, PO), and a hypoxic group treated with a high dose of DHA (hyp/DHA; 90 mg/kg, PO). The mice were maintained in a room at 20–24°C and 55%–65% humidity. The hypoxic groups were placed in a 10% hypoxic environment for 21 days at 24 hours per day.

Measurement of Hemodynamics and Right Ventricle Hypertrophy

Pressure transducers (PowerLab 8/35 Multichannel Biological Signal Recording System; AD Instruments, Australia) were used to record the hemodynamic index. The mice were anesthetized with 20% urethane (1 mL/100 g, ip). A catheter was inserted into the right ventricle (RV) through the right jugular vein to detect right ventricular systolic pressure (RVSP), which was assumed to be equivalent to pulmonary artery pressure. A catheter was inserted into the left carotid artery to detect the mean arterial pressure, which was assumed to be equivalent to systemic pressure. The ratio of the RV to the left ventricle (LV) and septum (S) represented the right ventricular hypertrophy index.

Measurement of Pulmonary Arterial Remodeling

Briefly, the connective tissue around the lung was removed, and 4% paraformaldehyde was used to fix the lung tissue for 24 hours. Lung tissue was then cut into 5-μm-thick slices after being embedded in paraffin. Sections were then stained with hematoxylin and eosin (HE), and an optical microscope was used to evaluate the structure of the pulmonary arteries with external diameters of 25–100 μm. Image-Pro Plus 6.0 (Media Cybernetics, Bethesda, MD) was used to analyze the ratio of the wall thickness (WT) to the total thickness (TT) and the pulmonary artery wall area (WA) to the total area (TA).

RNA Sequencing and Bioinformatics Analyses

Total RNA was extracted from each sample using TRIzol reagent (Invitrogen). RNA libraries were constructed using a NEBNext Ultra Directional RNA Library Prep Kit for Illumina (E7420L). cDNA libraries were constructed on a flow cell using an Illumina HiSeq sequencing platform at RIBOBIO (Guangzhou, China). Differential expression analysis was performed using the R package "Limma" with a cutoff P value of 0.05, and a cutoff |fold change| of 1.5. Heat maps and volcano plots were drawn on the dif-mRNA of the normoxic group versus the hypoxic group and the hypoxic group versus the hypoxic group treated with 90 mg/kg DHA using the "pheatmap" (https://cran.r-project.org/web/packages/pheatmap/index.html) and "ggplot2" R packages (https://cran.r-project.org/web/packages/ggplot2/).

qRT-PCR

mRNA and miRNA were isolated from mouse lung tissue and PASMCs using a UNIQ-10 Column TRIzol Total RNA Isolation Kit (Sangon Biotech, Shanghai, China). RNA was quantified using a UV-Vis spectrophotometer (NanoDrop, Thermo Fisher Scientific). To quantify miRNA, we used the miRNA First Strand cDNA Synthesis Kit (stem-loop method) and the miRNA qPCR Kit (Sangon Biotech). For reverse transcription and quantitative real-time PCR of mRNA, a qRT-PCR kit was purchased from Vazyme Biotech (Nanjing, China) and the process was performed using a CFX96 Real-Time PCR Detection System (Bio-Rad). The primer sequences used are listed in Table 1.

TABLE 1. The Sequence of Mimic, Inhibitor, siRNA, and Primers

Entry	Sequence
miR-503 mimic	Sense: GGAGUAUUGUUUCCGCUGCCUGG
	Antisense: CCAGGCAGCGGAAACAAUACUCC
miR-503 mimic negative control	Sense: UUUGUACUACACAAAAGUACUG
	Antisense: CAGUACUUUUGUGUAGUACAAA
miR-503 inhibitor	Sense: CCAGGCAGCGGAAACAAUACUCC
miR-503 inhibitor negative control	Sense: CAGUACUUUUGUGUAGUACAAA
siRNA- Elavl2-1	GGTCCAACCACTGTAAACA
siRNA- Elavl2-2	GCGAGATTGAGTCCTGTAA
siRNA- Elavl2-3	CTCTGAATGGATTGAGACT
siRNA negative control	GGCTCTAGAAAAGCCTATGC
U6 forward primer	AGAGAAGATTAGCATGGCCCCTG
U6 reverse primer	ATCCAGTGCAGGGTCCGAGG
U6 rt primer	GTCGTATCCAGTGCAGGGTCCGAGGTATTCGCACTGGATACGACAAAATA
rno-miR-503-5p forward primer	GAGCCTAGCAGCGGGAACAGTA
Reverse primer	CAGTGCAGGGTCCGAGGTAT
rt primer	GTCGTATCCAGTGCAGGGTCCGAGGTATTCGCACTGGATACGACCTGCAG
rACTB-F	AGCCATGTACGTAGCCATCC
rACTB-R	ACCCTCATAGATGGGCACAG

Preparation of Rat Primary PASMCs

Pulmonary arteries of rats anesthetized with 20% urethane (1 mL/100 g, i.p.) were isolated under a dissecting microscope. The separated and shredded pulmonary arteries were incubated with 0.2% type I collagenase (V900891; Merck) for 40 minutes at 37°C. After centrifugation, the cells were plated in a culture flask containing 500 μL fetal bovine serum.

Cell Culture

PASMCs from passages 4 to 6 were used to model hypoxia. Cells isolated from animals in the normoxic group were cultivated in a normal incubator with 21% O_2, 74% N_2, and 5% CO_2 at 37°C for 24 hours. Isolated cells in the hypoxic group were cultured in an incubator with 5% O_2, 90% N_2, and 5% CO_2 at 37°C for 24 hours.

Cell Transfection

The plasmid used for overexpression of *ELAVLL2* was purchased from Bio-report (Hangzhou, China), and small interfering RNA for knockdown of *ELAVLL2* was purchased from RiboBio (Guangzhou, China). Empty pCDNA3.1 and nontargeted control siRNA (siRNA NC) were used as negative controls. To overexpress or knock down miR-503, a mimic and inhibitor were purchased from RiboBio (Guangzhou, China). All the sequences of the constructs used in this study are listed in Table 1. Transfection of siRNA and the miRNA mimic and inhibitor was performed using Attractene Transfection Reagent (Qiagen, Hilden, Germany).

Cell Proliferation Assay

PASMCs were plated in 96-well plates at densities of 1000 cells/well. Drugs were administered and the hypoxia model was constructed the following day. On the third day, cell counting kit-8 (CCK8, Dojindo, Japan) reagent (10 μL) was used to detect cell viability. A 5-ethynyl-2′-deoxyuridine (EdU) cell proliferation assay kit (RiboBio, Guangzhou, China) was used to detect cell proliferation. EdU-positive cells (red fluorescence) and Hoechst 33,342-positive cells (blue fluorescence) were detected by fluorescence microscopy (Nikon eclipse Ti2, Japan), and their ratios were used to determine cell proliferation.

Transwell Migration Chamber Assay

Cells were added to the upper chamber of a Transwell migration assay system (8 μm, Corning Incorporated, NY) at a density of 5000 cells/well with 100 μL of Dulbecco's modified Eagle's medium, and Dulbecco's modified Eagle's medium containing 10% fetal bovine serum was added to the lower chamber. After 24 hours of incubation under normoxic or hypoxic conditions, cells were fixed in 4% paraformaldehyde and stained with crystal violet. Images of cells were obtained using a standard microscope (Leica DMi8, Germany).

Immunoblot Analysis

After lysis of PASMCs with radioimmunoprecipitation assay buffer, a BCA protein assay kit (Pierce Biotechnology, Rockford, IL) was used for protein quantification. Denatured proteins were separated using 10% SDS-PAGE and transferred to polyvinylidene fluoride membranes (Bio-Rad). The membranes were blocked with 5% nonfat milk for 1 hour and washed 3 times for 10 minutes in TBST. The membrane strips were incubated overnight with rabbit primary antibodies against PIK, p-AKT, AKT, PCNA, and β-actin. The next day, the strips were washed and incubated with goat antirabbit antibody labelled with horseradish peroxidase for 1 hour. A Bio-Rad ChemiDoc MP imaging system was used for imaging, and the Image Lab software (Bio-Rad) was used for quantification.

Dual-Luciferase Reporter Assay

PmiR-RB-ReportTM vectors with a putative miR-503 binding site or mutation were purchased from Bio-report (Hangzhou, China). Firefly luciferase (Luc) was used as the reporter and *Renilla* luciferase (Rluc) was used as the control. After transfection with 50 nM miR-503 mimic and 100 ng pmirGLO vector with Attractene transfection reagent, the cells were incubated for 48 hours, and luminescence was detected using the Dual-Luciferase Reporter Assay System (E1910, Promega).

RNA Binding Protein Immunoprecipitation Assay

A Magna RIP Kit was purchased from Millipore (Billerica, MA) to detect the binding between RNA and protein. Rat lung tissues were homogenized and lysed in RIP lysis buffer. An IgG antibody was used as the NC. The expression level of pre-miR-503 was determined using qRT-PCR.

Statistical Analysis

Student's *t*-test and one-way ANOVA followed by Tukey's post hoc test were performed using GraphPad Prism 7.0 (CA) to analyze single and multiple comparisons, respectively. The results are presented as mean ± SD. Differences were considered statistically significant at $P < 0.05$.

RESULTS

DHA Treatment Attenuated Hypoxia-Induced PH in Mice

First, we explored the therapeutic effects of DHA on hypoxia-induced PH in vivo. During the establishment of our model, no mice were found to have died from drug administration or environment. Hemodynamic results showed that the RVSP of mice under hypoxia was significantly increased, but the elevated RVSP was reduced upon treatment with DHA at a low concentration (45 mg/kg ig) or a high concentration (90 mg/kg ig) (Fig. 1A, C), whereas the mean arterial pressure among the 4 groups showed no significant differences (Fig. 1B, D). RV/WT, RV/(LV + S) and the absolute weight of RV increased under hypoxia and decreased after administration of DHA, proving the success of modeling and the therapeutic effect of DHA (Fig. 1E–G). Upon HE staining, the small pulmonary arterioles of hypoxic animals were found to be muscularized. This effect was reversed by treatment with low and high concentrations of DHA (Fig. 1H–J).

DHA Treatment Inhibited PASMC Migration and Proliferation

We used a PASMC model to explore whether DHA alleviates PH by inhibiting cell migration and proliferation. Transwell migration assays showed that the migration ability of PASMCs increased under hypoxic conditions, but this increase was inhibited by treatment with 5 μM and 10 μM DHA (Fig. 2A, B). The level of PCNA, an indicator of cell proliferation, significantly increased under hypoxic conditions, as demonstrated by western blotting. Treatment with DHA alleviated the hypoxia-induced proliferation effect, as shown in Figure 2C–E. Similar results were obtained using the EdU assay (Fig. 2F, G). Therefore, we concluded that DHA can inhibit hypoxia-induced migration and proliferation of PASMCs at concentrations of 5 μM and 10 μM.

miR-503 Inhibited PASMCs Migration and Proliferation by Inhibiting the PI3K/AKT Axis

Activation of the PI3K/AKT signaling pathway has been shown to contribute to cell proliferation in several diseases.[23,24] In addition, it has also been reported that miR-503 can inhibit MCT-induced PH in rats.[20] Therefore, we explored the potential interactions between miR-503 and PI3K. First, we predicted the potential targeting relationship between miR-503 and PI3K using TargetScan. This analysis suggested that miR-503 has good binding potential to the 3′-UTR of PI3K mRNA (Fig. 3A).

Therefore, to determine whether there was a targeting relationship between the 2, a dual-luciferase reporter assay was performed (Fig. 3B). First, we determined that the PI3K inhibitor, LY294002, reduced the viability of PASMCs under hypoxic conditions (Fig. 3C). In addition, western blot analysis demonstrated that overexpression of an miR-503 mimic resulted in a decrease in the expression level of PI3K protein (Fig. 3D). Accordingly, in the migration (Fig. 3E, F) and proliferation (Fig. 3G, H), we found that an miR-503 mimic had an inhibitory effect on the negative impact of hypoxia on PASMC growth, whereas the addition of the PI3K agonist 740Y-P reversed this inhibitory effect, compared with cells treated with LY294002. Furthermore, we found that miR-503 inhibited the migration and proliferation of PASMCs by downregulating PI3K to inhibit the phosphorylation and activation of AKT (Fig. 3I, J). It was concluded that miR-503 inhibits the proliferation and migration of PASMCs by inhibiting the PI3K/AKT axis.

MiR-503 Inhibited PASMCs Migration and Proliferation by Inhibiting the PI3K/AKT Axis

Next, we used qRT-PCR to explore whether the expression of miR-503 in PASMCs was altered upon treatment with DHA. As shown in Figure 4 A, the level of expression of miR-503 decreased under hypoxic conditions and increased upon treatment with DHA, indicating that DHA promoted the expression of miR-503. Transwell assays showed that the migration ability of PASMCs increased under hypoxic conditions and that this effect was reversed upon the addition of DHA. However, the addition of the miR-503 inhibitor reversed the migration inhibitory effect of DHA (Fig. 4B, D). Similar effects on proliferation were also observed via EdU assays (Fig. 4C, E).

We also examined the activation status of the PI3K/AKT pathway. Under hypoxia, the pathway was activated, as shown by an increase in PCNA expression, whereas the miR-503 inhibitor attenuated the proliferation inhibitory effect of DHA (Fig. 4F, G). In summary, DHA inhibited the migration and proliferation of PASMCs by regulating the miR-503/PI3K/AKT signaling pathway.

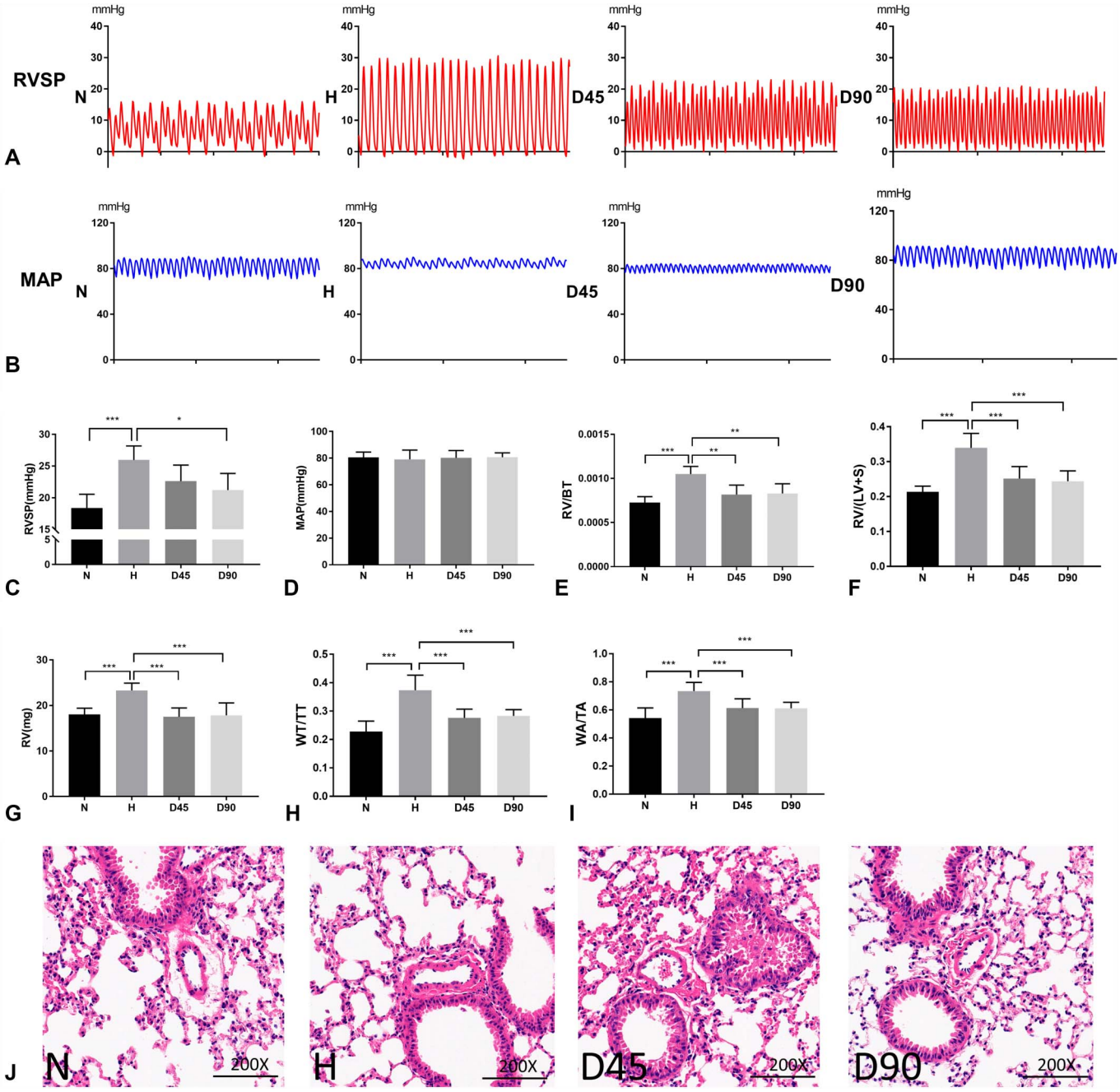

FIGURE 1. DHA treatment attenuated hypoxia-induced PH in mice. (A), (C), Representative images of RVSP waves for animals treated with normoxia (N), hypoxia (H), H with low DHA (45 mg/kg, D45) and H with high DHA (90 mg/kg, D90). Statistical graph of RVSP data for N, H, D45, and D90 groups (n = 6). (B), (D), Representative images of mean arterial pressure waves for animals treated with normoxia (N), hypoxia (H), H with low DHA (45 mg/kg, D45) and H with high DHA (90 mg/kg, D90). Statistical graph of mean arterial pressure data for N, H, D45 and D90 groups (n = 6). (E), (F), (G) RV hypertrophy shown as the right ventricle/body weight (RV/BT) ratios, the RV/(LV + S) and the absolute weight of RV (n = 6). (H), (I), The ratios of pulmonary artery wall thickness to total thickness (WT/TT) and wall area to total area (WA/TA) for each group (n = 6). J, Representative photomicrographs of HE staining for each group (×200; scale bar indicates 100 μm). Data are presented as the mean ± SD. $*P < 0.05$; $**P < 0.01$; *** $P < 0.001$; NS, not significant.

ELAVL2 Was Identified as a Key RBP in PH

To explore the molecular mechanism underlying the regulation of PASMC migration and proliferation by DHA through miR-503, samples of lung tissue from mice treated under normoxic and hypoxic conditions and hypoxic mice treated with 90 mg/kg DHA were used for mRNA high-

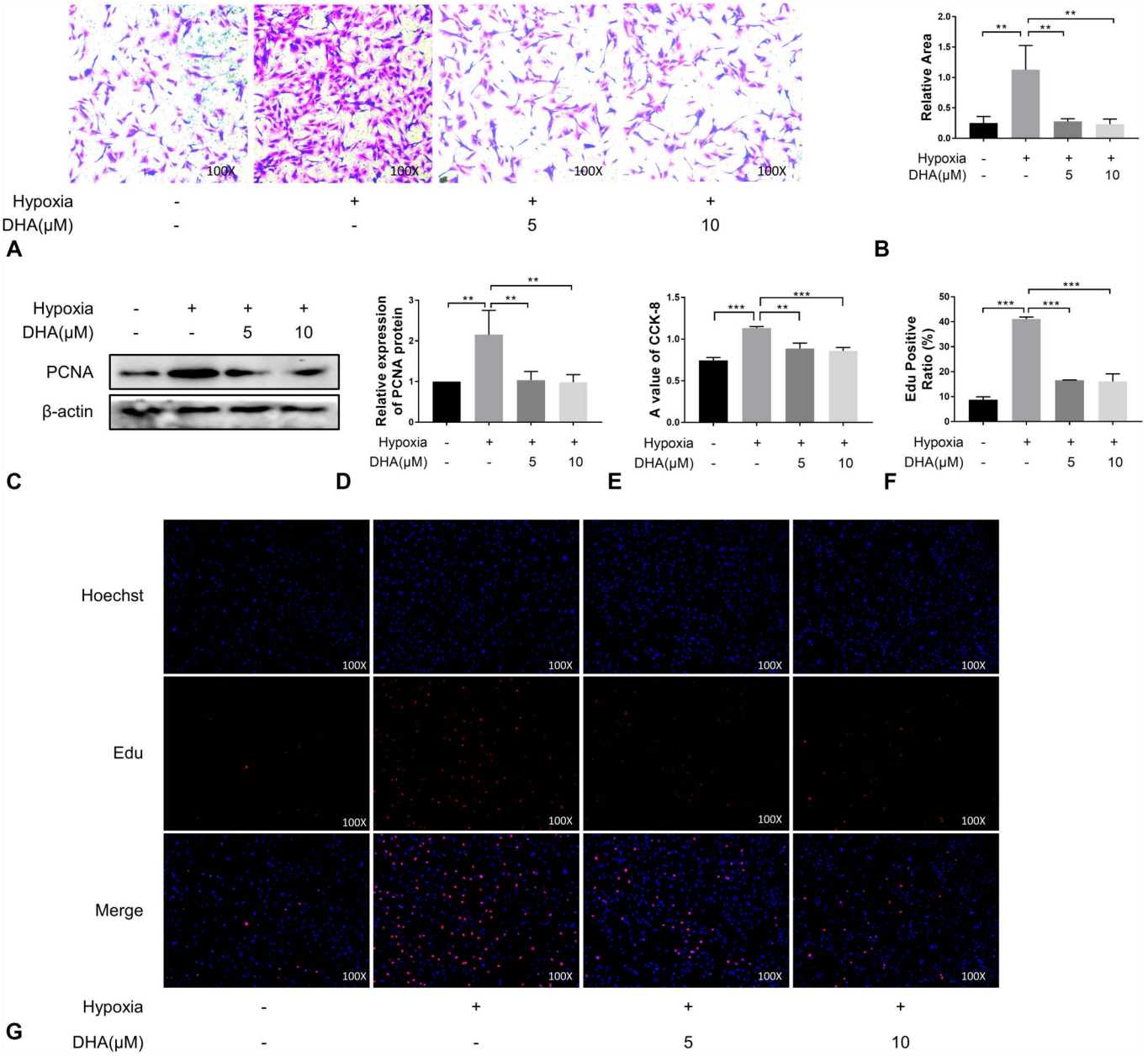

FIGURE 2. DHA treatment inhibited PASMC migration and proliferation. (A), (B), Cell migration was determined by transwell assays at 24 hours (n = 3) (×100). (C), (D), Immunoblotting analysis of PCNA expression in PASMCs of each group (n = 3). E, CCK-8 experiment (n = 6). (F), (G), EdU incorporation experiments (n = 3) were used to evaluate cell viability (×100).

throughput sequencing. As shown in the heat map and volcano map, 901 differentially expressed mRNAs were found in normoxic mice compared with hypoxic mice (Fig. 5A, B), and 14,857 differentially expressed mRNAs were found in hypoxic mice compared with hypoxic mice treated with 90 mg/kg DHA (Fig. 5C, D). After identifying the intersection of these genes, 370 genes were found to be differentially expressed among the 3 groups (Fig. 5E). These 370 genes were compared with a library of RBPs from a previous study.[25] This analysis led to the identification of a single RBP, ELAVL2, that may play an essential role in PH (Fig. 5F).

ELAVL2 Negatively Regulates PASMC Migration and Proliferation

Although ELAVL2 was originally identified as a neuron-specific protein, it has recently been found to function more widely in other tissues and cells.[26–28] In view of the low expression of ELAVL2 in mice treated under hypoxic conditions, we overexpressed it to explore its function (Fig. 6A, C). We found that ELAVL2 overexpression inhibited the hypoxia-induced increase in migration (Fig. 6B, D) and proliferation (Fig. 6E, F) of PAMSCs. A subsequent decrease in PI3K, p-AKT, AKT, and PCNA levels after ELAVL2

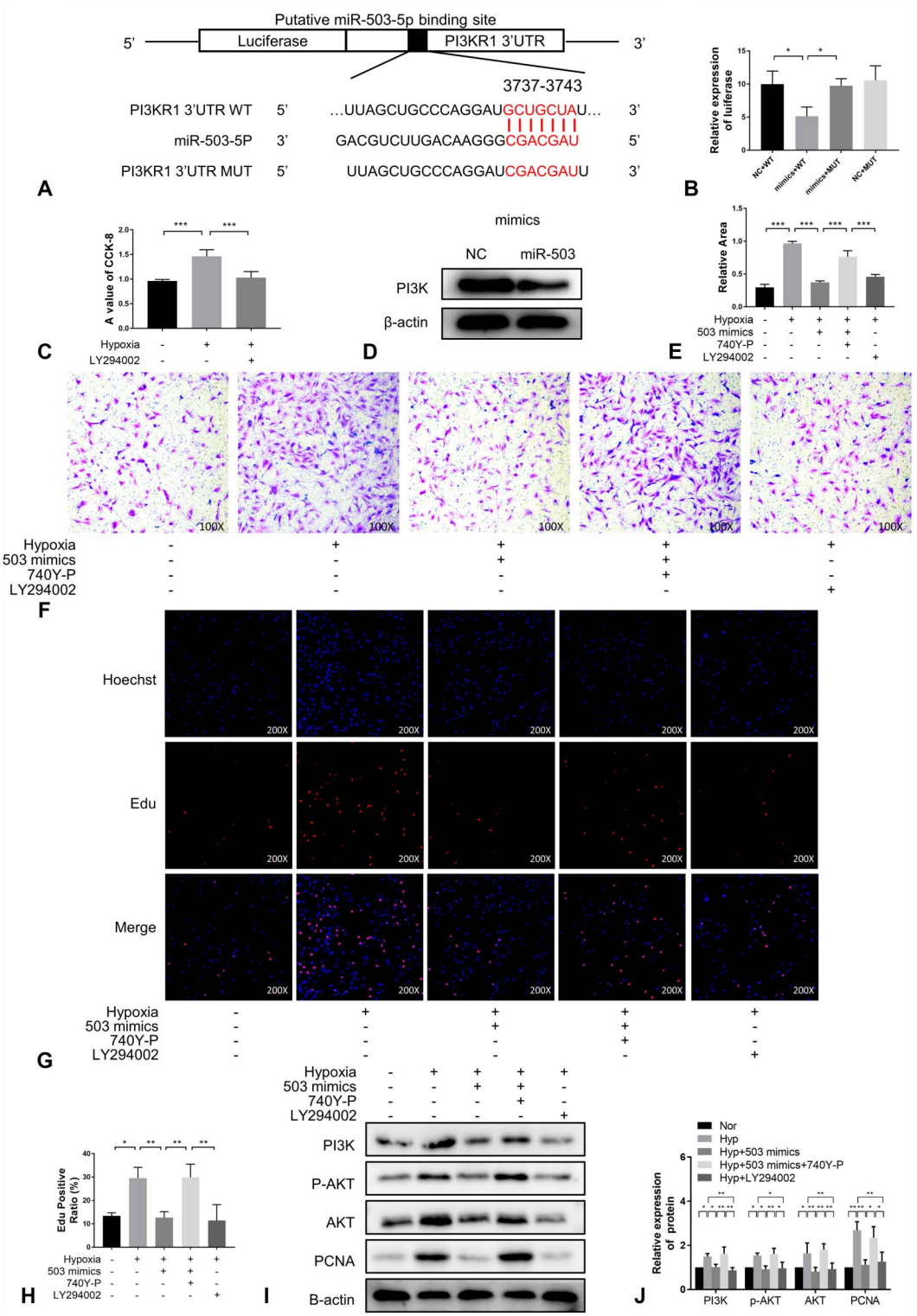

FIGURE 3. MiR-503 inhibited PASMC migration and proliferation by inhibiting the PI3K/AKT axis. A, The potential target sites of miR-503 matching the 3′-UTR of PI3K. B, Compared with the negative control (WT + negative control), when miR-503 was added to wild-type (WT) PI3K, it inhibited luciferase activity, whereas miR-503 had no effect on mutant PI3K (n = 6). C, CCK-8 experiment (n = 6). (D), (G), Cell migration was determined by transwell assays at 24 hours (n = 3) (×100). E, Immunoblotting analysis of PI3K expressions in PASMCs of each group (n =3). (F), (H), EdU incorporation experiment (n = 3) were used to evaluate cell viability (×200). (I), (J), Immunoblotting analysis of the expression of PI3K, AKT, p-AKT and PCNA in PASMCs from each treatment group (n = 3).

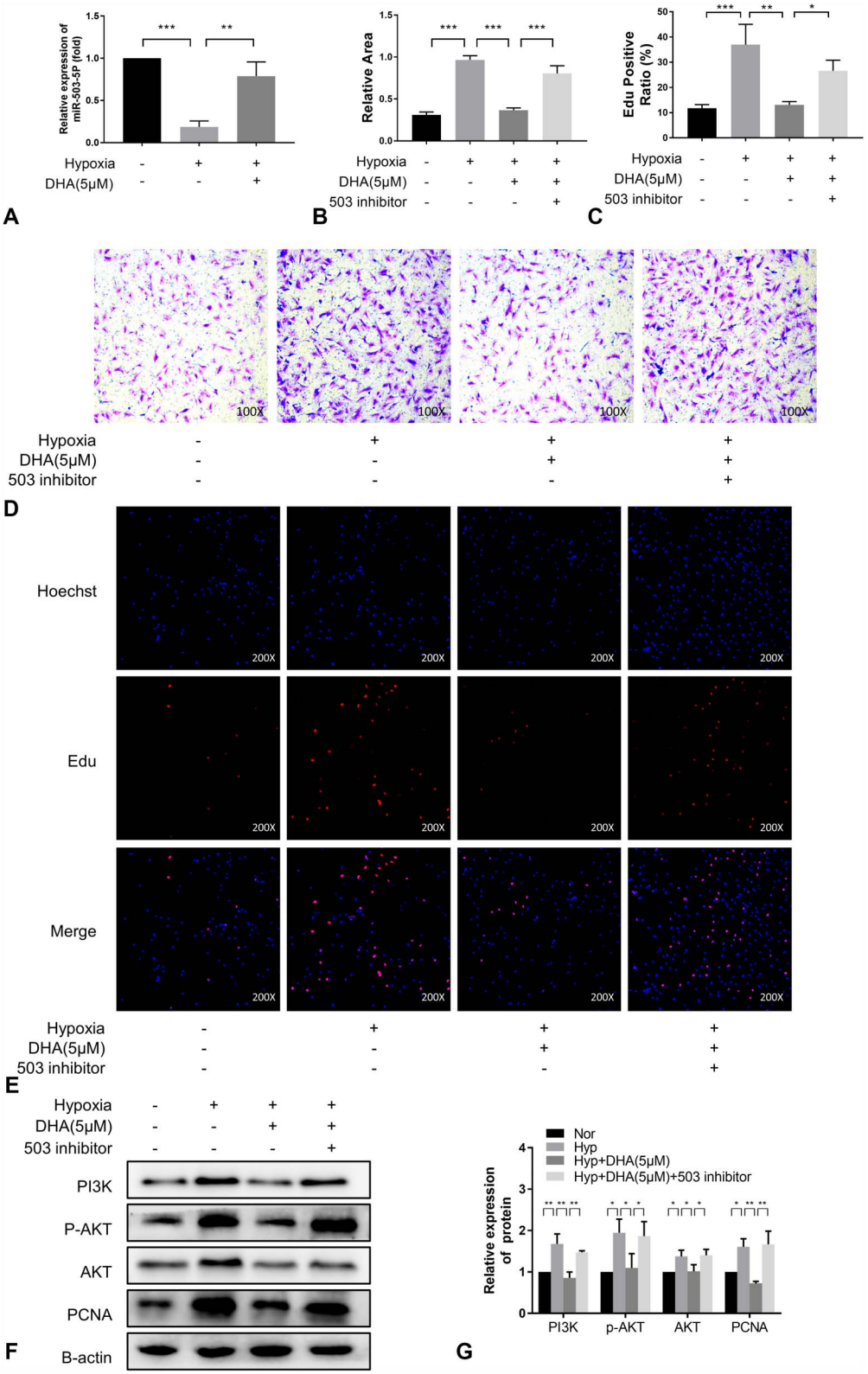

FIGURE 4. MiR-503 inhibited PASMCs migration and proliferation by inhibiting the PI3K/AKT axis. A, MiR-503 expression in rat PASMCs of each treatment group was measured by qRT-PCR (n = 3). (B), (D), Cell migration was determined by transwell assays at 24 hours (n = 3) (×100). (C), (E), EdU incorporation experiments (n = 3) were used to evaluate cell viability (×200). (F), (G), Immunoblotting analysis of the expression of PI3K, AKT, p-AKT and PCNA in PASMCs from each treatment group (n = 3).

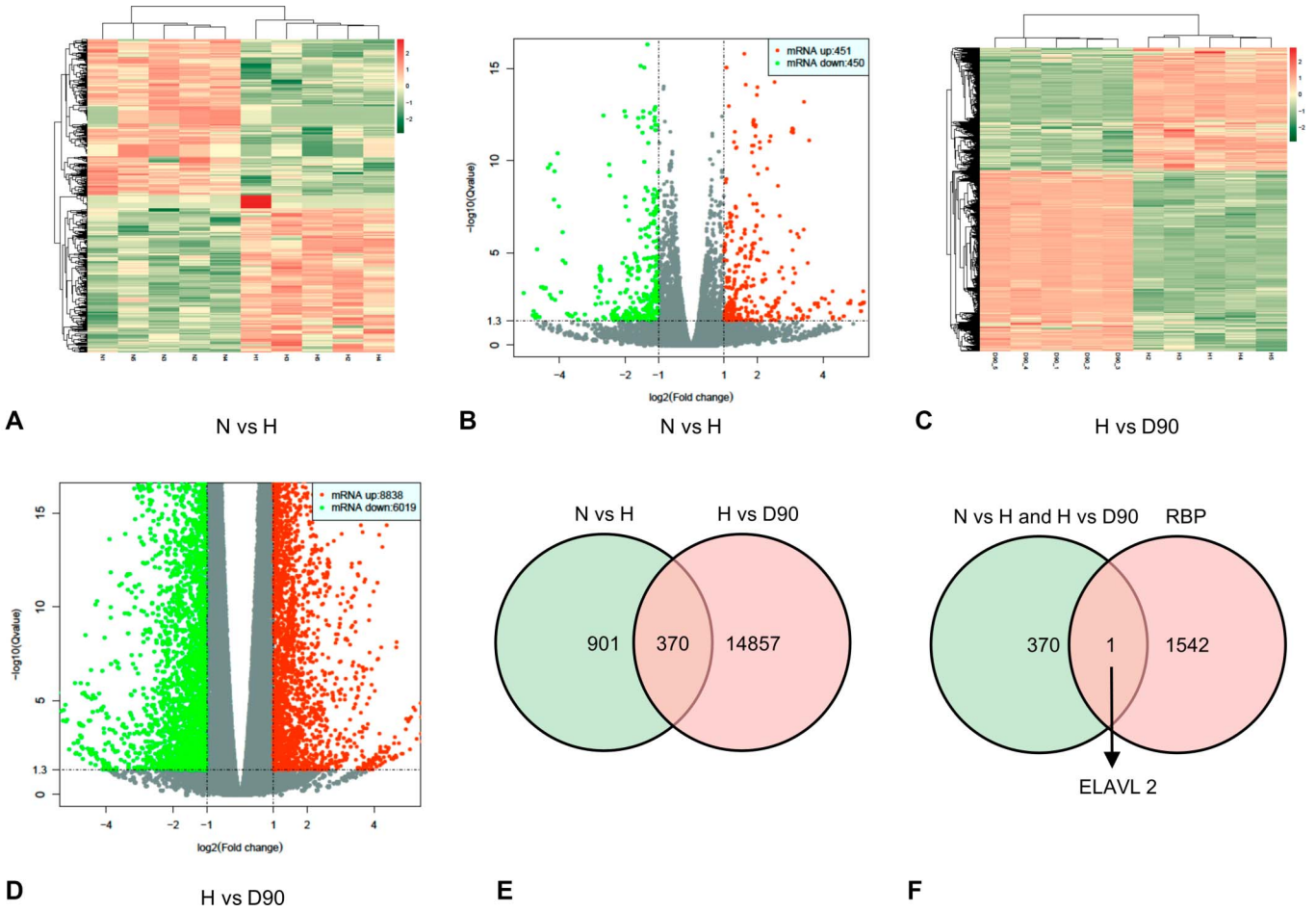

FIGURE 5. ELAVL2 was identified as a key RBP in PH. (A), (B), Heat map diagram and volcano plots demonstrating differential mRNA expression of the normoxia group (N group) versus hypoxia group (H group). (C), (D), Heat map diagram and volcano plots demonstrating differential mRNA expression of hypoxia group (H group) versus H + DHA (90 mg/kg, D90) groups. (E), Venn diagram showing 370 differential mRNA expressions that were upregulated or downregulated in the 3 treatment groups. F, Venn diagram showing that ELAVL2 is represented among the 370 differential mRNAs and in a previously reported RBP library.

overexpression also confirmed this finding (Fig. 6G, H). Therefore, we conclude that ELAVL2 regulates hypoxia-induced migration and proliferation of PASMCs.

DHA Inhibits PASMCs Migration and Proliferation by Up-Regulating ELAVL2

We tested the hypothesis that DHA functions via ELAVL2 by knocking down ELAVL2 expression. We tested multiple siRNA sequences for knockdown efficiency and found that siRNA-3 had the best knockdown efficiency for ELAVL2 (Fig. 7A–C). Consistent with previous observations, the migration (Fig. 7D, E) and proliferation (Fig. 7F, G) of PASMCs increased under hypoxic conditions, and these increases were inhibited by treatment with DHA. However, the therapeutic effect of DHA was abrogated by transfection with siRNA-3. The results of western blot analyses were consistent with these findings. The levels of PI3K, p-AKT, AKT, and PCNA increased under hypoxia and were reversed after DHA administration. SiRNA-3 of ELAVL2 reversed the reversal effect of DHA (Fig. 7H, I). These results demonstrate that the therapeutic effect of DHA on PASMCs was achieved through interaction with ELAVL2.

The Therapeutic Effect of ELAVL2 in PH Is Mediated through miR-503

These results suggested a connection between ELAVL2 and miR-503. Therefore, this potential connection was investigated by qRT-PCR analysis of miR-503 expression. Here, we found that miR-503 was down-regulated upon the knockdown of ELAVL2 (Fig. 8A). In addition, RBP immunoprecipitation assay demonstrated a direct interaction between ELAVL2 and pre-miR-503 (Fig. 8B). At the cellular level, the inhibition of hypoxia-induced migration (Fig. 8C, D) and proliferation (Fig. 8E, F) of PASMCs by the overexpression of ELAVL2 was reversed by the inhibitor of miR-503. Together, these results indicate that miR-503 is a downstream target of ELAVL2 and that this interaction is mediated by pre-miR-503.

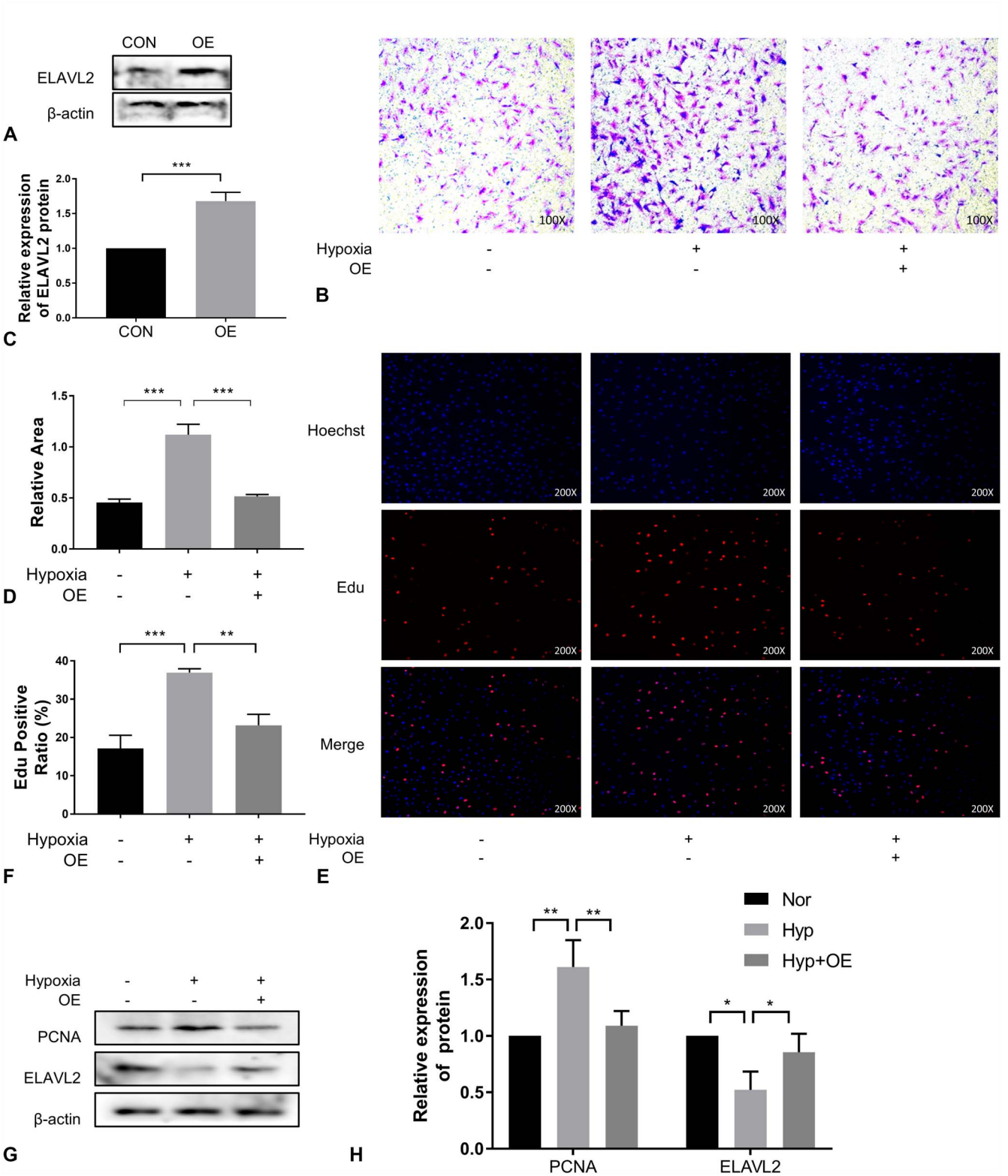

FIGURE 6. ELAVL2 regulated PASMCs migration and proliferation negatively. (A), (B), Immunoblotting analysis of ELAVL2 expression in PASMCs transfected with an ELAVL2-overexpressing plasmid or a control plasmid (n =3). (C), (D), Cell migration was determined by transwell assays at 24 hours (n = 3) (×100). (E), (F), EdU incorporation experiments (n = 3) were used to evaluate cell viability (×200). (G), (H), Immunoblotting analysis of ELAVL2 and PCNA expression in PASMCs of each treatment group (n = 3). OE means overexpression of ELAVL2.

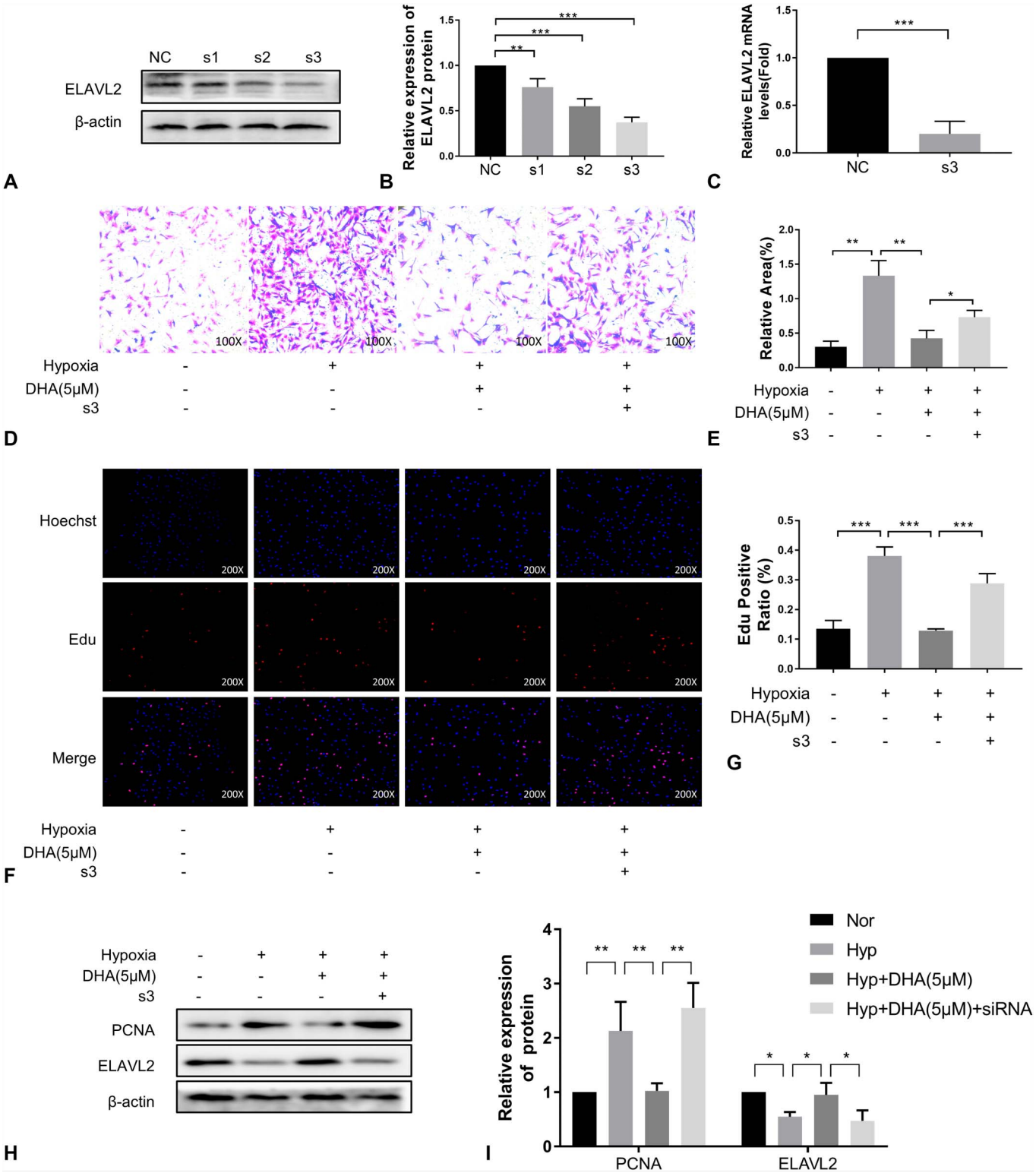

FIGURE 7. DHA inhibits PASMCs migration and proliferation by up-regulating ELAVL2. (A), (B), Immunoblotting analysis of ELAVL2 expression in PASMCs to which ELAVL2 siRNA or a negative control siRNA were added (n =3). C, ELAVL2 expression in rat PASMCs of each treatment group was measured by qRT-PCR (n = 3). (D), (E), Cell migration was determined by transwell assays at 24 hours (n = 3) (×100). (F), (G), EdU incorporation experiments (n = 3) were used to evaluate cell viability (×200). (H), (I), Immunoblotting analysis of ELAVL2 and PCNA expression in PASMCs of each treatment group (n = 3).

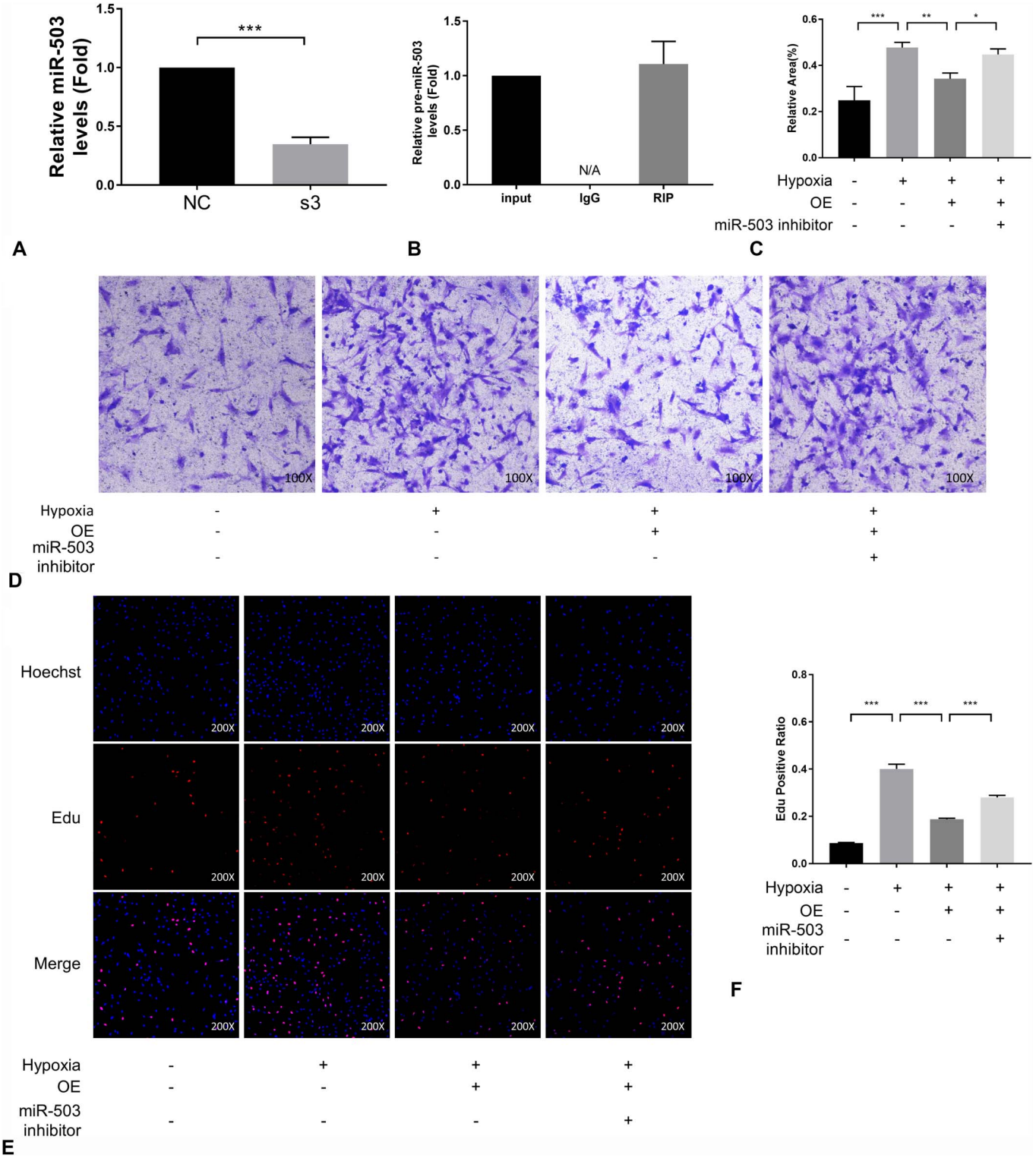

FIGURE 8. The therapeutic effect of ELAVL2 in PH acted through miR-503. A, miR-503 expression in rat PASMCs to which ELAVL2 siRNA or control siRNA was transfected was measured by qRT-PCR (n = 3). B, An RBP immunoprecipitation assay was performed to investigate the binding of ELAVL2 to pre-miRNA-503. Results were quantified by qRT-PCR (n = 3). (C), (D), Cell migration was determined by transwell assays at 24 hours (n = 3) (×100). (E), (F), EdU incorporation experiment (n = 3) were used to evaluate cell viability (×200). OE means overexpression of ELAVL2.

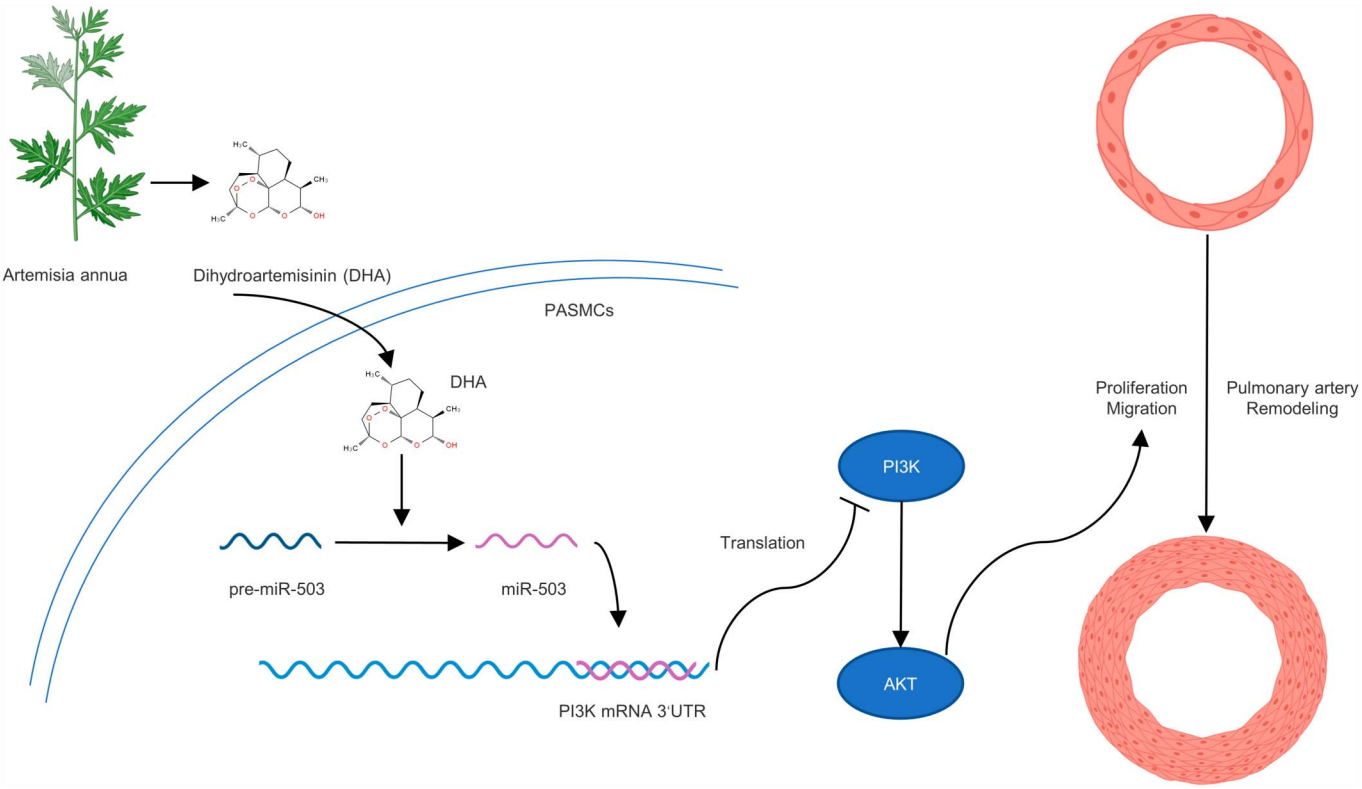

FIGURE 9. DHA inhibits the proliferation and migration of PASMCs through the ELAVL2/miR-503/PI3K/AKT axis.

DISCUSSION

Among the various pathologic factors in the pathogenesis of PH, chronic hypoxia is one of the key factors, especially in chronic obstructive pulmonary disease, restrictive lung diseases, and high-altitude PH. Our study focused on the role of chronic hypoxia in PH. Hypoxia-induced PH mouse models are widely used in studies.[29,30] The pathologic features of this model are pulmonary artery remodeling, elevated pulmonary artery pressure, and right ventricular hypertrophy. In our study, the increase in RVSP, RV/(LV + S), WA/TA (%), and WT/TT (%) and the muscularization of small arteries, as shown by HE staining, demonstrated the successful establishment of a PH model in mice kept under hypoxic conditions for 21 days.

Artemisinin, a natural product extracted from the leaves of *A. annua*, has been used to treat malaria.[31] Recently, additional evidence has suggested that artemisinin and its derivatives may be effective in the treatment of various cancers,[32] inflammatory diseases[33] and other ailments. DHA is a first-generation derivative of artemisinin with high biological activity.[34] In this study, we provided the first evidence that DHA inhibits the proliferation and migration of PASMCs through the ELAVL2/miR-503/PI3K/AKT axis (Fig. 9).

First, we showed that DHA attenuated hypoxia-induced PH in vivo. The reduction in RVSP, RV/(LV + S), WA/TA (%), and WT/TT (%) and improvement of vascular muscularization in pathologic sections with DHA treatment verified the therapeutic effect of DHA on PH in vivo. To explore the molecular mechanism of DHA in PH, we demonstrated the therapeutic properties of DHA at the cellular level through experiments related to the migration and proliferation of PASMCs. In particular, miR-503, which acts as a protective factor in PH, aroused our interest. As reported previously, the rescue of miR-503 in PAECs suppressed the proliferation of PASMCs induced by the media of PAECs. Moreover, overexpression of miR-503 effectively inhibited and reversed MCT-induced PH in rats.[20] This evidence suggests that miR-503 is a protective factor in PH. The targeting relationship of miR-503 to *PI3K* mRNA has been elucidated in detail in various diseases, such as pulmonary fibrosis,[21] but this link remains unproven in PH. Our study demonstrated the pro-expression effect of DHA on miR-503 and the prodegradation effect of miR-503 on PI3K mRNA in PH.

Intriguing is how DHA is linked to miR-503. After being transcribed in the nucleus, miRNA transcripts are spliced into shorter sequences, miRNA precursors (pre-miRNAs), which are then transported to the cytoplasm. In the cytoplasm, pre-miRNAs are cleaved into mature forms by dicer.[35] In the above process, any intervention will lead to changes in the final expression level of miR-503. ELAVL2 belongs to the ELAVL protein family, which was originally characterized as an RBP that is indispensable for the development of the nervous system.[15] ELAVL proteins typically stabilize transcripts through AU-rich elements to increase protein expression.[36] In previous models, ELAVL protein and miRNAs were believed to antagonistically regulate downstream mRNAs or cooperatively downregulate the expression of mRNAs.[37] In a 2017 study, ELAVL2 was found to interact

with more than 50 miRNA precursors.[18] However, the role of ELAVL2 in PH and how ELAVL2 regulates miR-503 are unknown. Therefore, it is meaningful to explore the potential regulatory mechanisms in PH. We focused on the functions of ELAVL2, which is expressed at low levels under hypoxic conditions, in PASMCs. Our experimental results showed that miR-503 changed in the same direction as ELAVL2 after ELAVL2 downregulation, suggesting that ELAVL2 exists in the upstream of miR-503 and has a positive regulatory effect on miR-503. The results of the RNA-binding protein immunoprecipitation assay showed the binding of ELAVL2 and pre-miR-503, indicating that pre-miR-503 may be a node regulated by ELAVL2 considering the cytoplasmic location of ELAVL2.[38] However, how ELAVL2 binds directly or indirectly to pre-miR-503 remains to be explored. The binding site between the 2 requires further exploration. We propose that dicer1-mediated processing of pre-miRNAs may be a potential regulatory target; further research is required to clarify the specific mechanism.

Undoubtedly, RBPs are important players in PH. Some of them have been validated in PH patients, such as SRSF2[39] and TLR3.[40] An increasing number of studies have demonstrated the potential therapeutic value of RBPs in PH. And we propose for the first time that DHA can regulate ELAVL2 in PH. In a hypoxic model of human pulmonary arterial endothelial cells, DHA has been reported to effectively inhibit hypoxia-induced cell proliferation, migration and oxidative stress, which is achieved by promoting autophagy.[14] In a rat PH model induced by MCT, DHA reduced the mean pulmonary arterial pressure and attenuates pulmonary vascular remodeling.[13] Although the mechanism still needs further study, the above studies and our results are sufficient to show that DHA is a Chinese medicinal monomer with potentiality, which may provide reference for clinical treatment of PH. We also recognized that the study would be more convincing if clinical samples were available.

CONCLUSIONS

DHA reduces the hypoxia-induced migration and proliferation of PASMCs through promoting the expression of miR-503 in PH. This beneficial effect is produced by the inhibition of PI3K mRNA and downstream AKT activation. Acting as a mediator connecting DHA and miR-503, ELAVL2, whose low expression under hypoxia is reversed by DHA, positively regulates miR-503. Our research proved the protective effect of ELAVL2 in PH for the first time, and we demonstrated a novel relationship between ELAVL2 and miR-503. We confirmed that DHA inhibits the proliferation and migration of PASMCs through the ELAVL/miR-503/PI3K/AKT axis. This research provides new insights and perspectives on the role of RBPs and miRNAs in PH and provides an experimental basis for the clinical treatment of PH.

AVAILABILITY OF DATA AND MATERIAL

All data are presented in the article. Original data supporting the conclusions of this study are available from the authors.

STATEMENT OF ETHICS

All animal procedures conformed to the guidelines of Directive 2010/63/EU of the European Parliament on the conservation of animals used for scientific purposes or the current NIH guidelines and were approved by the Animal Ethics Committee of Wenzhou Medical University. During the study, all animals were carefully handled and euthanized.

ACKNOWLEDGMENTS

The authors thank the Key Laboratory of Heart and Lung of Wenzhou Medical University for their support with this study.

REFERENCES

1. Southgate L, Machado RD, Gräf S, et al. Molecular genetic framework underlying pulmonary arterial hypertension. *Nat Rev Cardiol.* 2020;17:85–95.
2. Thenappan T, Ormiston ML, Ryan JJ, et al. Pulmonary arterial hypertension: pathogenesis and clinical management. *BMJ.* 2018;360:j5492.
3. Thompson AAR, Lawrie A. Targeting vascular remodeling to treat pulmonary arterial hypertension. *Trends Mol Med.* 2017;23:31–45.
4. Bisserier M, Katz MG, Bueno-Beti C, et al. Combination therapy with STAT3 inhibitor enhances SERCA2a-induced BMPR2 expression and inhibits pulmonary arterial hypertension. *Int J Mol Sci.* 2021;22:9105.
5. Qin Y, Qiao Y, Li L, et al. The m(6) A methyltransferase METTL3 promotes hypoxic pulmonary arterial hypertension. *Life Sci.* 2021;274:119366.
6. Hu L, Wang J, Huang H, et al. YTHDF1 regulates pulmonary hypertension through translational control of MAGED1. *Am J Respir Crit Care Med.* 2021;203(9):1158–1172.
7. Dasgupta A, Chen KH, Lima PDA, et al. PINK1-induced phosphorylation of mitofusin 2 at serine 442 causes its proteasomal degradation and promotes cell proliferation in lung cancer and pulmonary arterial hypertension. *FASEB J.* 2021;35:e21771.
8. Lin AJ, Lee M, Klayman DL. Antimalarial activity of new water-soluble dihydroartemisinin derivatives. 2. Stereospecificity of the ether side chain. *J Med Chem.* 1989;32:1249–1252.
9. Zhang B, Chen X, Gan Y, et al. Dihydroartemisinin attenuates benign prostatic hyperplasia in rats by inhibiting prostatic epithelial cell proliferation. *Ann Transl Med.* 2021;9:1246.
10. Du J, Wang X, Li Y, et al. DHA exhibits synergistic therapeutic efficacy with cisplatin to induce ferroptosis in pancreatic ductal adenocarcinoma via modulation of iron metabolism. *Cell Death Dis.* 2021;12:705.
11. Wang Y, Li Z, Teng M, et al. Dihydroartemisinin inhibits activation of the AIM2 inflammasome pathway and NF-κB/HIF-1α/VEGF pathway by inducing autophagy in A431 human cutaneous squamous cell carcinoma cells. *Int J Med Sci.* 2021;18:2705–2715.
12. Zheng J, Li X, Yang W, et al. Dihydroartemisinin regulates apoptosis, migration, and invasion of ovarian cancer cells via mediating RECK. *J Pharmacol Sci.* 2021;146:71–81.
13. Tang M, Wang R, Feng P, et al. Dihydroartemisinin attenuates pulmonary hypertension through inhibition of pulmonary vascular remodeling in rats. *J Cardiovasc Pharmacol.* 2020;76:337–348.
14. Yu H, Liu J, Dong Y, et al. Anti-hypoxic effect of dihydroartemisinin on pulmonary artery endothelial cells. *Biochem Biophys Res Commun.* 2018;506:840–846.
15. Good PJ. A conserved family of elav-like genes in vertebrates. *Proc Natl Acad Sci U S A.* 1995;92:4557–4561.
16. Brennan CM, Steitz JA. HuR and mRNA stability. *Cell Mol Life Sci.* 2001;58:266–277.
17. Hambardzumyan D, Sergent-Tanguy S, Thinard R, et al. AUF1 and Hu proteins in the developing rat brain: implication in the proliferation and differentiation of neural progenitors. *J Neurosci Res.* 2009;87:1296–1309.
18. Treiber T, Treiber N, Plessmann U, et al. A compendium of RNA-binding proteins that regulate MicroRNA biogenesis. *Mol Cel.* 2017;66:270.e13–284.e13.

19. Bartel DP. MicroRNAs: genomics, biogenesis, mechanism, and function. *Cell*. 2004;116:281–297.
20. Kim J, Kang Y, Kojima Y, et al. An endothelial apelin-FGF link mediated by miR-424 and miR-503 is disrupted in pulmonary arterial hypertension. *Nat Med.* 2013;19:74–82.
21. Yan W, Wu Q, Yao W, et al. MiR-503 modulates epithelial-mesenchymal transition in silica-induced pulmonary fibrosis by targeting PI3K p85 and is sponged by lncRNA MALAT1. *Sci Rep.* 2017;7:11313.
22. Yi L, Liu J, Deng M, et al. Emodin inhibits viability, proliferation and promotes apoptosis of hypoxic human pulmonary artery smooth muscle cells via targeting miR-244-5p/DEGS1 axis. *BMC Pulm Med.* 2021;21:252.
23. Liu M, Yang P, Fu D, et al. Allicin protects against myocardial I/R by accelerating angiogenesis via the miR-19a-3p/PI3K/AKT axis. *Aging (Albany NY).* 2021;13:22843–22855.
24. Mao G, Mu Z, Wu DA. Exosomal lncRNA FOXD3-AS1 upregulates ELAVL1 expression and activates PI3K/Akt pathway to enhance lung cancer cell proliferation, invasion, and 5-fluorouracil resistance. *Acta Biochim Biophys Sin (Shanghai).* 2021;53:1484–1494.
25. Gerstberger S, Hafner M, Tuschl T. A census of human RNA-binding proteins. *Nat Rev Genet.* 2014;15:829–845.
26. Yang C, Yao C, Ji Z, et al. RNA-binding protein ELAVL2 plays post-transcriptional roles in the regulation of spermatogonia proliferation and apoptosis. *Cell Prolif.* 2021;54:e13098.
27. Li S, Yang Q, Zhou Z, et al. SNHG3 cooperates with ELAVL2 to modulate cell apoptosis and extracellular matrix accumulation by stabilizing SNAI2 in human trabecular meshwork cells under oxidative stress. *Environ Toxicol.* 2021;36:1070–1079.
28. Kato Y, Iwamori T, Ninomiya Y, et al. ELAVL2-directed RNA regulatory network drives the formation of quiescent primordial follicles. *EMBO Rep.* 2019;20:e48251.
29. Berghausen EM, Janssen W, Vantler M, et al. Disrupted PI3K subunit p110α signaling protects against pulmonary hypertension and reverses established disease in rodents. *J Clin Invest.* 2021;131:e136939.
30. Luo L, Chen Q, Yang L, et al. MSCs therapy reverse the gut microbiota in hypoxia-induced pulmonary hypertension mice. *Front Physiol.* 2021;12:712139.
31. Woodrow CJ, Haynes RK, Krishna S. Artemisinins. *Postgrad Med J.* 2005;81:71–78.
32. Efferth T, Dunstan H, Sauerbrey A, et al. The anti-malarial artesunate is also active against cancer. *Int J Oncol.* 2001;18:767–773.
33. Xu H, He Y, Yang X, et al. Anti-malarial agent artesunate inhibits TNF-alpha-induced production of proinflammatory cytokines via inhibition of NF-kappaB and PI3 kinase/Akt signal pathway in human rheumatoid arthritis fibroblast-like synoviocytes. *Rheumatology (Oxford).* 2007;46:920–926.
34. Tu Y. The development of the antimalarial drugs with new type of chemical structure–qinghaosu and dihydroqinghaosu. *Southeast Asian J Trop Med Public Health.* 2004;35:250–251.
35. Woldemariam NT, Agafonov O, Høyheim B, et al. Expanding the miRNA repertoire in atlantic salmon; discovery of IsomiRs and miRNAs highly expressed in different tissues and developmental stages. *Cells*. 2019;8:42.
36. Toba G, White K. The third RNA recognition motif of Drosophila ELAV protein has a role in multimerization. *Nucleic Acids Res.* 2008;36:1390–1399.
37. Srikantan S, Tominaga K, Gorospe M. Functional interplay between RNA-binding protein HuR and microRNAs. *Curr Protein Pept Sci.* 2012;13:372–379.
38. Okano HJ, Darnell RB. A hierarchy of Hu RNA binding proteins in developing and adult neurons. *J Neurosci.* 1997;17:3024–3037.
39. Cogan J, Austin E, Hedges L, et al. Role of BMPR2 alternative splicing in heritable pulmonary arterial hypertension penetrance. *Circulation*. 2012;126:1907–1916.
40. Farkas D, Thompson AAR, Bhagwani AR, et al. Toll-like receptor 3 is a therapeutic target for pulmonary hypertension. *Am J Respir Crit Care Med.* 2019;199:199–210.